RESEARCH MEMORANDUM

ARRANGEMENT OF BODIES OF REVOLUTION IN SUPERSONIC FLOW TO REDUCE WAVE DRAG

By Morris D. Friedman

Ames Aeronautical Laboratory
Moffett Field, Calif.

NATIONAL ADVISORY COMMITTEE
FOR AERONAUTICS

WASHINGTON
December 17, 1951

National Aeronautics and
Space Administration

Langley Research Center
Hampton, Virginia
23665

NASA

Reply to Attn of 139A

JUN 1 6 1983

TO: Distribution

FROM: 180A/Security Classification Officer

SUBJECT: Authority to Declassify NACA/NASA Documents Dated Prior to January 1, 1960

Effective this date, all material (informal correspondence) classified by this Center prior to January 1, 1960, is declassified. This action does not include material derivatively classified at the Center upon instructions from other Agencies.

Immediate re-marking is not required; however, until material is re-marked by lining through the classification and annotating with the following statement, it must continue to be protected as if classified:

> "Declassified by authority of LaRC Security Classification Officer (SCO) letter dated June 16, 1983," and the signature of person performing the re-marking.

If re-marking a large amount of material is desirable, but unduly burdensome, custodians may follow the instructions contained in NHB 1640.4, subpart F, section 1203.604, paragraph (h).

This declassification action complements earlier actions by the National Archives and Records Service (NARS) and by the NASA Security Classification Officer (SCO). In Declassification Review Program #07008, NARS declassified the Center's "Research Authorization" files, which contain reports, Research Authorizations, correspondence, photographs, and other documentation. Earlier, in a 1971 letter, the NASA SCO declassified all NACA/NASA formal series documents with the exception of the following reports, which must remain classified:

Document No.	First Author
E-51A30	Nagey
E-53G20	Francisco
E-53G21	Johnson
E-53K18	Spooner
SL-54J21a	Westphal
E-55C16	Fox
E-56H23a	Himmel

JUN 2 3 1983

If you have any questions concerning this matter, please call Mr. William L. Simkins at extension 3281.

Jess G. Ross
2898

Distribution:
SDL 031

cc:
NASA Scientific and Technical
Information Facility
P.O. Box 8757
BWI Airport, MD 21240

NASA--NIS-5/Security
180A/RIAD
139A/TU&AO
139A/WLSimkins:elf 06/15/83 (3281)
139A/JS 6-15-83

31-01 HEADS OF ORGANIZATIONS
HESS, JANE S.,
MAIL STOP 163 BLDG 1194

NATIONAL ADVISORY COMMITTEE FOR AERONAUTICS

RESEARCH MEMORANDUM

ARRANGEMENT OF BODIES OF REVOLUTION IN SUPERSONIC FLOW TO REDUCE WAVE DRAG

By Morris D. Friedman

Summary

The wave drag of a combination of slender bodies of revolution at zero angle of attack is studied with a view to determining the arrangements for which the total drag is a minimum. Linearized theory is used to calculate the pressure distribution in the field surrounding the bodies. The interference drag coefficient is computed for different arrangements.

The special cases of two bodies and of a three-body combination with bilateral symmetry are considered. The bodies treated are of the form determined by Sears and Haack as having minimum wave drag for prescribed volume and length. They also have equal fineness ratios. Numerical calculations of the drag coefficient of interference are carried out and curves are drawn which show the relative positions at which minimum drag occurs.

A three-body configuration is found for which the total wave drag is about 35 percent less than the sum of the individual wave drags of the three bodies.

INTRODUCTION

The drag of a body of revolution in supersonic flow has been considered by von Kármán, Haack (references 1 and 2), and others. Haack and Sears (references 2 and 3) have determined theoretical body shapes for which the wave or pressure drag is a minimum. Such bodies have important present-day flight applications since this wave drag, as an additional form of drag at supersonic speeds, limits the performance of modern aircraft.

If, in respect to the wave drag, the components of an aircraft such as the fuselage and wing-tip tanks and nacelles, say, are replaced by equivalent bodies of revolution, then the question of the combined wave

drag is of interest. Different arrangements of the bodies of revolution at zero angle of attack are investigated and that combination which has the smallest combined wave drag is determined. A practical combination would consist of a large body or fuselage and/or two smaller bodies which could represent either wing nacelles or tip tanks. In particular, the drag coefficient for the case of two slender bodies of equal fineness ratio (ratio of total length to maximum diameter) and unequal lengths is considered. (See fig. 1.) The procedure to be outlined, however, permits generalization, for the body shape chosen, to any number of bodies of any relative size.

SYMBOLS

a	speed of sound
b	abscissa of center of body of revolution
c	constant, the value of which determines the fineness ratio $\left(\frac{R_{max}^2}{m^3}\right)$
C_{D_I}	coefficient of interference drag $\left(\frac{D_I}{q_o S}\right)$
C_{D_t}	drag coefficient of the configuration based on the total frontal area of the configuration
C_p	pressure coefficient
D_I	drag change due to interaction of body pressure fields
E	complete elliptic integral of the second kind of modulus k
E_o	$\frac{2}{\pi} E$
F_o	$\frac{2}{\pi} K$
K	complete elliptic integral of the first kind of modulus k
k	modulus of the complete elliptic integrals
L	path of integration
m	half-length of body
M	Mach number $\left(\frac{V}{a}\right)$

q_o	free-stream dynamic pressure
r	cylindrical coordinate $(\sqrt{y^2 + z^2})$
r_o	particular value of r
R	radius of a section
R_{max}	radius of maximum section
S	cross-sectional area of body or bodies
V	free-stream velocity
x,y,z	rectangular coordinates
β	$\sqrt{M^2 - 1}$
ζ	argument of the elliptic integrals of the third kind
Λ_o	term which occurs in the circular case of the elliptic integral of the third kind
ξ	dummy variable of integration
φ	perturbation velocity potential

Subscripts

1	parent body
2	satellite body
I,II,III	regions of integration
t	combination as a whole

GENERAL CONSIDERATIONS

The type of configuration studied is illustrated in figure 1. It consists of a large and a small body each of the form having minimum wave drag for given volume and length and each of the same fineness ratio. The large body is situated on the axis with its center at the origin. The smaller body has its axis parallel to the axis of the large body and

may be within the flow field of the large body. The equation for the shape of such bodies, which may be supposed to be created by distributing sources and sinks along an axis, is given by Haack (reference 2) as

$$R^2 = c\,[m^2 - (x-b)^2]^{3/2} \qquad (1)$$

with $b = 0$ for the parent and $b = b$ for the satellite body. (For $b = 0$, this formula is the expression for a thin body of revolution of length $2m$ with center at the origin and fineness ratio $2m/2R_{max}$.)

To calculate the interference drag of such a configuration, two possibilities must be considered:

1. Only one of the bodies is within the disturbed flow field of the other.

2. Each body is in the disturbed flow field from the other.

When one of the bodies lies within the disturbed flow field of the other, the effects of the flow field in which this body is located must be considered. In other words, if all or part of either body is behind the Mach wave from the nose of the other body the streamlines will be distorted and a pressure will be exerted by the flow field of one body on the other.

The potential field which results from the interaction of the flow fields consists of the sum of the individual potentials and an interference potential. In the cases when there are multiple reflections between the bodies a series of interference potentials may occur. Since the interference potentials are usually of higher order of smallness, they will be assumed negligible. Of course, at very high Mach numbers, or when the bodies are relatively close to each other, the effect of this interference may not be negligible.

The interference drag coefficient due to the location of a body in the flow field of another can be evaluated by integrating the product of the additional, disturbed, pressure at a point and the slope of the body surface at that point. In a similar manner, the interference drag coefficient for the case when each body lies within the disturbed flow field of the other can be calculated.

As a preliminary step, therefore, it is necessary to find an expression for the pressure around each body for the whole region behind the Mach wave from the nose of the body.

METHOD OF CALCULATION

The Pressure Field Surrounding A Single Body

Under the assumptions of linearized theory, the shape of a slender body of revolution is described by the distribution along an axis of sources and sinks which satisfy the potential equation and the boundary conditions of uniform flow at infinity. Under these assumptions the source strength is given by

$$2\pi f'(x) = V\frac{d^2S}{dx^2}$$

where S is the expression for the area of a section.

The pressure coefficient, in this theory, is found from the relation

$$C_p = -\frac{2}{V}\frac{\partial \varphi}{\partial x} \tag{2}$$

where, as given in reference 2, $\partial\varphi/\partial x$ is given by

$$\frac{\partial \varphi}{\partial x} = -\int_{\text{nose}}^{x-\beta r} \frac{f'(\xi)d\xi}{\sqrt{(x-\xi)^2 - \beta^2 r^2}} \tag{3}$$

Here

$$f'(\xi) = \frac{-3c}{2}V\left[\frac{m^2 - 2(\xi-b)^2}{\sqrt{m^2 - (\xi-b)^2}}\right]$$

is the expression for the source strength in terms of the following coordinates of integration:

$$\beta^2 = M^2 - 1$$

$$r^2 = y^2 + z^2$$

When $f'(\xi)$ is replaced in equation (3) by its equivalent, and the substitution is made for $\partial\varphi/\partial x$ in equation (2), the pressure coefficient is found to be determined by the integral

$$C_p = -3c\int_L \frac{[m^2 - 2(\xi-b)^2]d\xi}{\sqrt{[m^2 - (\xi-b)^2][(x-\xi)^2 - \beta^2 r^2]}} \tag{4}$$

This integral is elliptic, and the limits of integration and the method of solution depend on the following three regions (see fig. 2):

Region I is bounded by the Mach aftercone from the nose and the Mach forecone from the tail. The limits of integration are b-m and x-βr.

Region II is bounded by the Mach forecone from the tail and the Mach aftercone from the tail. The limits of integration again are b-m and x-βr.

Region III is bounded by the Mach aftercone from the tail and infinity. The limits of integration are b-m and b+m.

With these limits the elliptic integrals for the different regions are complete and the solutions are:[1]

Region I

$$C_p = \frac{-3\pi c}{2\sqrt{(m+\beta r)^2 - (x-b)^2}}\left\{[m^2 + 2\beta r(m+b-x) - 2(x-b)^2]\, F_o(k_I) - \right.$$

$$[(m+\beta r)^2 - (x-b)^2]\, E_o(k_I) +$$

$$\left. 2(x-b)\sqrt{(m+\beta r)^2 - (x-b)^2}\, \Lambda_o(k_I, \zeta_I) \right\} \qquad (5)$$

where

$$k_I = \sqrt{\frac{(m-\beta r)^2 - (x-b)^2}{(m+\beta r)^2 - (x-b)^2}}; \quad \zeta_I = \sin^{-1}\sqrt{\frac{m+\beta r+x-b}{2m}}$$

and the change of variable

$$u = sn^{-1}\sqrt{\frac{(m+\beta r+b-x)(\xi+m-b)}{(m-\beta r-b+x)(m+b-\xi)}}$$

transforms equation (4) into normal elliptic form.

[1]Solution of these integrals was accomplished with the aid of a table of elliptic integrals compiled by Mr. Paul F. Byrd of the Ames Aeronautical Laboratory.

Region II

$$C_p = \frac{-3\pi c}{2\sqrt{m\beta r}} \left\{ m(m+2\beta r+2b-2x)F_o(k_{II}) - 4m\beta r E_o(k_{II}) + 4(x-b)\sqrt{m\beta r}\ \Lambda_o(k_{II}, \zeta_{II}) \right\} \tag{6}$$

where

$$k_{II} = \sqrt{\frac{(x-b)^2 - (m-\beta r)^2}{4m\beta r}}; \quad \zeta_{II} = \sin^{-1}\sqrt{\frac{2m}{x-b+\beta r+m}}$$

and the change of variable

$$u = sn^{-1}\sqrt{\frac{2\beta r(\xi-b+m)}{(x-b-\beta r+m)(x+\beta r-\xi)}}$$

transforms equation (4) into normal elliptic form.

Region III

$$C_p = \frac{+3\pi c}{\sqrt{(x-b)^2 - (m-\beta r)^2}} \left\{ (x-b-\beta r)^2 F_o(k_{III}) + [(x-b)^2 - (m-\beta r)^2] \right.$$

$$\left. [E_o(k_{III})] - 2(x-b)\sqrt{(x-b)^2 - (m-\beta r)^2}\ \Lambda_o(k_{III}, \zeta_{III}) \right\} \tag{7}$$

where

$$k_{III} = \sqrt{\frac{4\beta rm}{(x-b)^2 - (m-\beta r)^2}}; \quad \zeta_{III} = \sin^{-1}\sqrt{\frac{x+\beta r-m-b}{x+\beta r+m-b}}$$

and the change of variable

$$u = sn^{-1}\sqrt{\frac{(x+\beta r-m-b)(\xi-b-m)}{2m(x+\beta r-\xi)}}$$

transforms equation (4) into normal elliptic form.

The functions F_o, E_o, and Λ_o are tabulated in reference 4, where they are also defined as:

$$F_o(k) = \frac{2}{\pi}K(k)$$

$$E_o(k) = \frac{2}{\pi}E(k)$$

$$\Lambda_o(k,\zeta) = E_o(k)F(k',\zeta) + F_o(k)E(k',\zeta) - F_o(k)F(k',\zeta)$$

where

$K(k)$ complete elliptic integral of the first kind of modulus k

$E(k)$ complete elliptic integral of the second kind of modulus k

$F(k',\zeta)$, $E(k',\zeta)$ incomplete elliptic integrals of the first and second kind of modulus k' $(= \sqrt{1-k^2})$, and argument ζ, respectively

Thus, according to linearized theory, equations (5), (6), and (7) completely determine the pressure field in the region behind the Mach wave from the nose of a body of revolution of the prescribed shape. An isometric sketch of the pressure coefficient at fixed values of the radial distance is shown in figure 3.

Interference Drag Coefficient

An inspection of figure 3 shows that the gradient of the curve of the pressure coefficient in the stream direction changes from negative to positive behind the center of the body. This region of positive pressure gradients is a zone of favorable buoyancy in the pressure field around the body. Therefore, a small body placed anywhere within this zone should have a negative interference drag (i.e., a thrust) due to this pressure field which should cause a decrease in the combined drag.

If the pressure coefficient surrounding a body at a given lateral distance $r = r_o$ be called C_{p_t}, the interference drag coefficient may then be calculated from the expression

$$C_{D_I} = \frac{1}{\pi R_{max}^2}\int_{nose}^{tail} C_{p_t}\, 2\pi \frac{R\,dR}{dx}\,dx \qquad (8)$$

where R_{max} is the radius of the frontal area of the reference body. Substitution of the respective values for the quantities in equation (8) yields

$$C_{D_I} = \frac{1}{\pi R_{max}^2} \int_{b-m}^{b+m} C_{p_t} \left\{ -3\pi c\,(x-b) \sqrt{m^2 - (x-b)^2} \right\} dx \qquad (9)$$

Actually, the integral in equation (8) or (9) is made up of one or more integrals depending on the number of regions in which the small body is located. The limits of integration depend on the parameters b, m, r, and β which determine the regions of integration. This integral must be computed numerically.

For a clearer exposition of the mathematical computations in the cases where interference exists, it is necessary to distinguish between the bodies. In the present case, if the central body situated on the x axis be denoted by the subscript 1 and the other body by the subscript 2, then, depending on which body is being acted upon, the interference drag coefficient is

$$C_{D_I} = \frac{1}{\pi R_{max}^2} \int_{b_2-m_2}^{b_2+m_2} C_{p_{t_1}} \left\{ -3\pi c_2 (x-b_2) [m_2^2 - (x-b_2)^2]^{1/2} \right\} dx \qquad (10)$$

or

$$C_{D_I} = \frac{1}{\pi R_{max}^2} \int_{b_1-m_1}^{b_1+m_1} C_{p_{t_2}} \left\{ -3\pi c_1 (x-b_1) [m_1^2 - (x-b_1)^2]^{1/2} \right\} dx \qquad (11)$$

Equations (10) and (11) are, to a first approximation, the drag coefficients due to the effect of body 1 on 2 and body 2 on 1, respectively. The integration extends from the nose to the tail of the body which is in the disturbed flow field. Similarly, for the calculation, to a first approximation, of the drag coefficients due to the interaction of the bodies, formulas (10) and (11) are both used.

The preceding equations permit the calculation of the interference drag coefficient for any arrangement of bodies. In particular, equations (10) and (11) apply to the special case when two identical bodies are symmetrically placed with respect to a central body so that each body may be in the flow field of the others. The formulas may be applied to any configuration, whatever the interference pattern.

[redacted]

Numerical Calculations

As an exploratory investigation, the simple case of a small body having one-half the length of the large body was chosen. This combination is derived by assigning the following values to the parameters in equation (1):

c	m	b
$c_1 = 0.005$	$m_1 = 2$	$b_1 = 0$
$c_2 = .01$	$m_2 = 1$	$b_2 = b$

The equations which describe the bodies are

$$R_1^2 = 0.005\,(4-x^2)^{3/2}$$

$$R_2^2 = .01\,[1-(x-b)^2]^{3/2}$$

It is to be noted that each body has the fineness ratio 10 but that one is twice as long as the other.

The pressure coefficient depends on β and r_o. The dependence is on βr_o, rather than on either parameter individually, and the calculations were carried out for $\beta r_o = 0.5m_2$, $1.0m_2$, and $2.0m_2$; where, as shown previously $m_2 = 1$. A change in β and in r_o which keeps βr_o invariant will not change the calculations.

The drag coefficient, with respect to the frontal area, of the individual body is given by Haack (reference 1) as $\frac{9\pi^2}{8}\left(\frac{R_{max}}{m}\right)^2$, or in this case $\frac{0.09\pi^2}{8}$. The interference drag coefficient is computed from formula (9). For each value of βr_o, therefore, the remaining parameter b, in this case the longitudinal distance between the centers of the bodies, is given values between $-3m_2$ and $+4m_2$.

The interference drag coefficients based on frontal area of the small body are sketched for different $\frac{\beta r_o}{m_2}$ and $\frac{b}{m_2}$ in figure 4. Since the reversibility of drag (reference 5) holds true, the curves would be expected to be symmetrical about the line $\frac{b}{m_2} = 0$ (where $\frac{b}{m_2}$ is the nondimensional longitudinal distance between the centers of the bodies). The symmetry in the figure is a measure of the accuracy of the numerical calculations. From the figure, it is evident that minimum drag occurs when the small body is close to the large one $\left(\frac{\beta r_o}{m_2} = 0.5\right)$ and with its center just forward of the tail wave from the large body.

It may be observed that, while the interference drag varies markedly with fore and aft position, for the range of βr_o considered the maximum favorable interference that can be obtained generally decreases with increasing separation between the bodies. It is interesting to note that drag minimums occur whenever the center of the satellite body is just forward of the tail Mach wave of the parent body. Also of interest is the fact that, in the case when both bodies had their centers on the vertical axis, the lowest drag occurred when the lateral separation parameter (βr_o) was equal to the length of the small body and higher drags resulted as the bodies were brought closer together.

In figure 5, there are plotted the values of the total drag coefficient, based on the total frontal area of a three-body combination with bilateral symmetry, against the longitudinal distance between the centers of the parent and satellite bodies. Since interaction between all three bodies occurred only for the lowest value of βr_o ($= 0.5m_2$) where it was found to be negligible, the interference drag coefficients previously calculated for the two-body configuration could be used directly to determine the total drag of the three-body configuration. As a consequence, the variations in drag coefficient are similar to those of figure 4. Again the lowest drag occurred at $\beta r_o = 0.5m_2$ and was approximately 35 percent less than the drag of the three bodies without interference.

Because of the unusual shapes of the curves in figure 4, it was considered advisable to investigate the drag interaction of a combination of bodies of different shape. The slender pointed body derived by Jones and Margolis (reference 6) was selected for this purpose since for the same fineness ratio the drag coefficient is comparable to that of the Sears-Haack body. The interference drag coefficients of a combination of two such bodies with $m_1/m_2 = 2$ were calculated for $b = 0$, and different values of βr_o. Reasonable agreement was obtained with the results of figure 4 for $\beta r_o = 2.0m_2$ and $\beta r_o = 1.0m_2$. In the case when $\beta r_o = 0.5m_2$, since the bodies are close together, there is a discrepancy which may be due to the differences in body geometry.

CONCLUDING REMARKS

It is found that the combined wave drag of a combination of bodies of revolution can be decreased if an arrangement is chosen which takes advantage of a favorable pressure zone which exists behind the center of each body.

In the cases discussed, where the ratio of the lengths of the bodies was 2 to 1 but the fineness ratios were equal, numerical calculations showed that the maximum favorable interference occurred when the

center of the small body was just forward of the stern Mach wave from the large body and the bodies were close together. For the range of βr_o considered the magnitude of the favorable interference generally decreased with increasing separation between the bodies.

In the case of a bilaterally symmetrical arrangement of three bodies with a lateral separation equal to one-quarter of the length of the small body the total wave drag was found to be 35 percent less than the combined wave drag of the three bodies.

National Advisory Committee for Aeronautics
Ames Aeronautical Laboratory
Moffett Field, Calif., Sept. 20, 1951

REFERENCES

1. von Kármán, Th.: The Problem of Resistance in Compressible Fluids. GALCIT Pub. No. 75, 1936 (From R. Acad. D'Italia; cl. scie, fis. mat. e nat., vol XIV, 1936)

2. Haack, W.: Projectile Shapes for Smallest Wave Drag. Brown Univ. Trans. A9-T-3, Grad. Div. App. Math., 1948.

3. Sears, William R.: On Projectiles of Minimum Wave Drag. Quart. App. Math., vol. IV, no. 4, Jan. 1947, pp. 361-366.

4. Heuman, Carl: Tables of Complete Elliptic Integrals. Jour. Math. and Phys., vol 19-20, 1940-41, pp. 127-206.

5. Hayes, Wallace D.: Linearized Supersonic Flow. Calif. Inst. Tech. Thesis, June 1947. North American Aviation, Inc., Rept. AL-222.

6. Jones, Robert T., and Margolis, Kenneth: Flow Over a Slender Body of Revolution at Supersonic Velocities. NACA TN 1081, 1946.

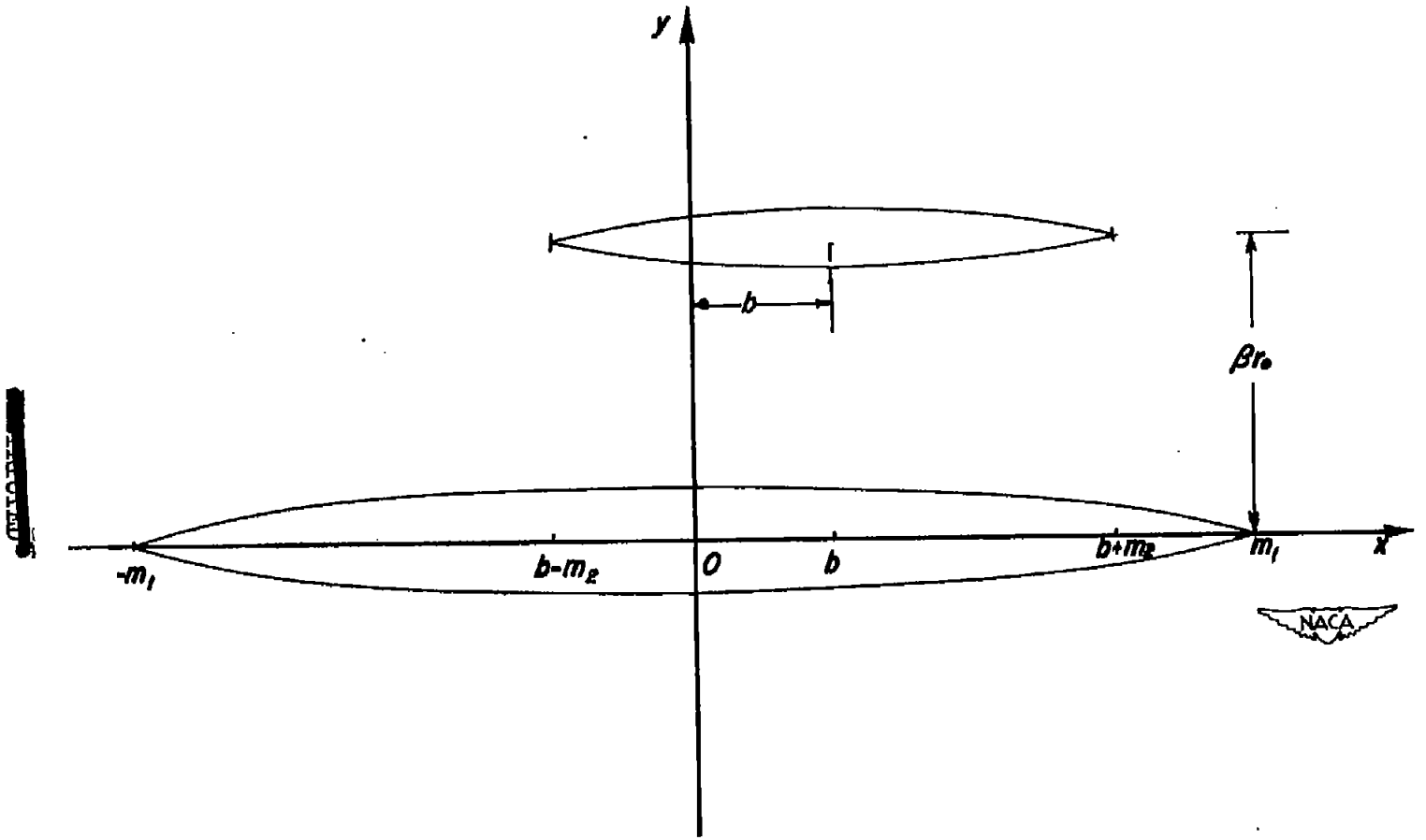

Figure I.- Coordinate system.

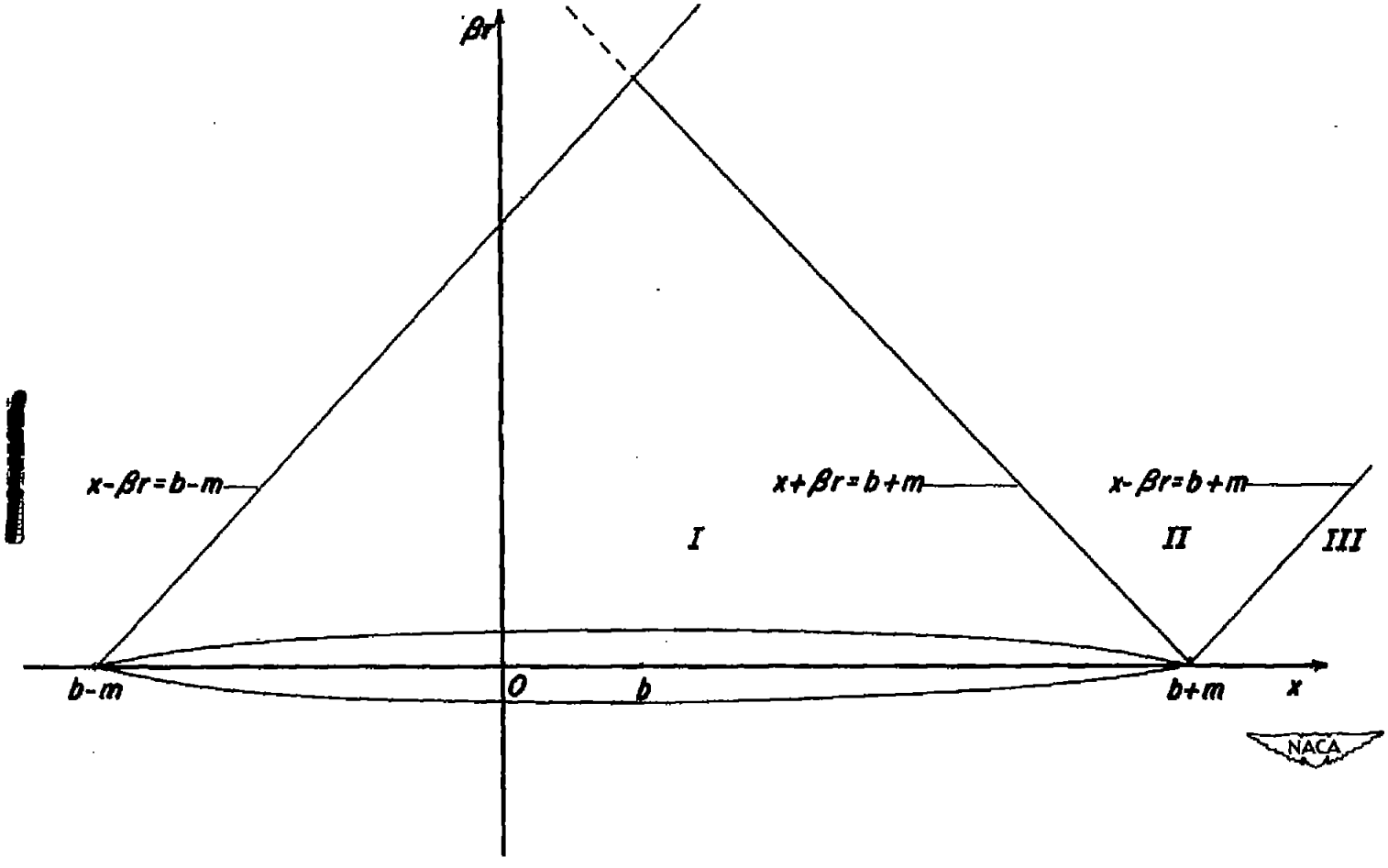

Figure 2.- Regions of integration.

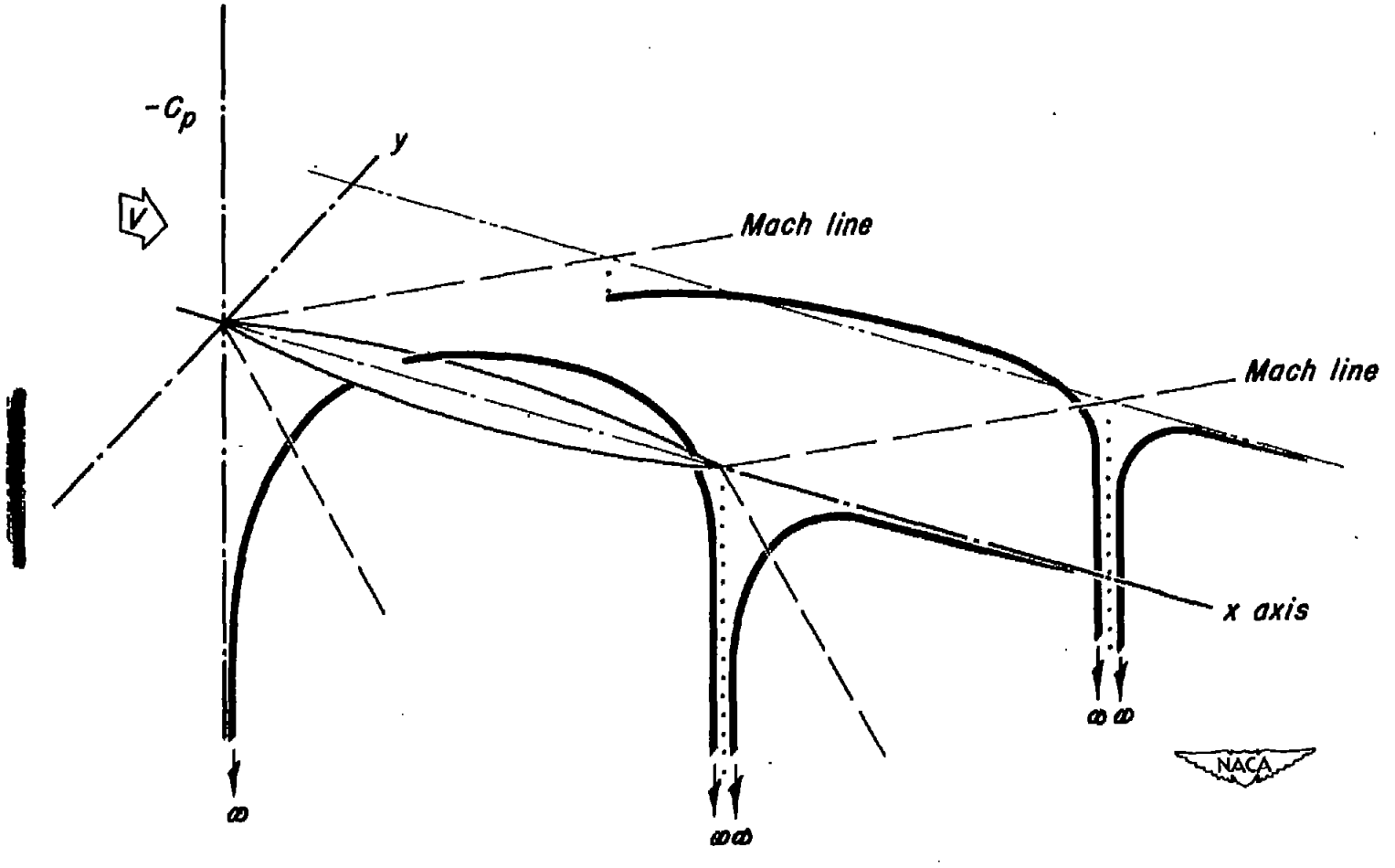

Figure 3.- Isometric sketch of the pressure distribution in the field surrounding a single body.

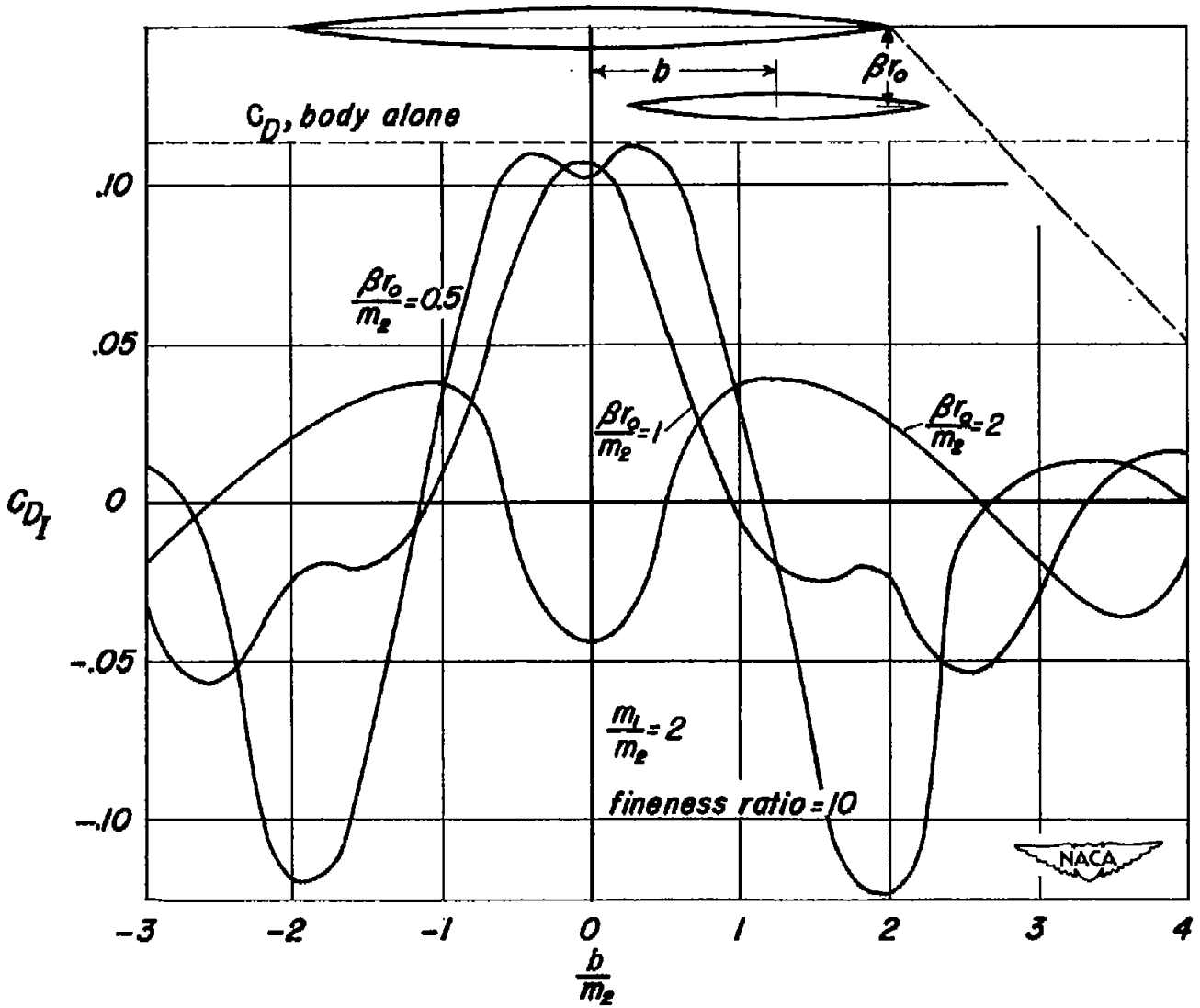

Figure 4.– Interference drag coefficient of configuration based on the area of the small body.

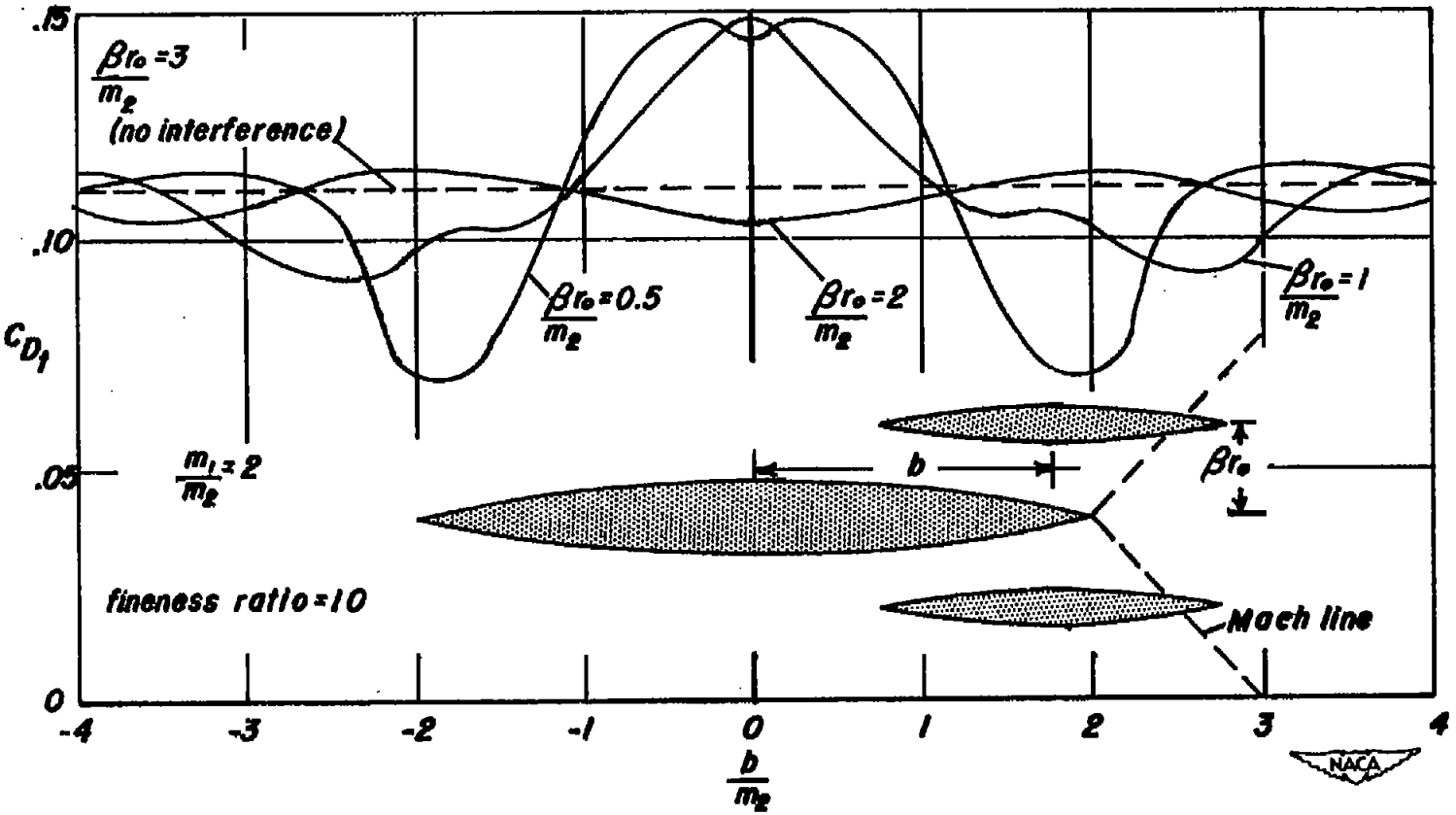

Figure 5.- Total drag coefficient of three-body combination with bilateral symmetry.